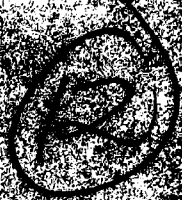




**LEVEL** *JP*



AFTR-78-88-24  
Technical Report  
January 1980

ADA 084349

**A STUDY OF REAL TIME SIGNAL  
PROCESSING METHODS FOR DECODING  
SPREAD SPECTRUM SYSTEMS**

**Aerodyne Research Inc.**

H. J. Caulfield  
Robert Haines  
Peter Mueller

APPROVED FOR PUBLIC RELEASE; DISTRIBUTION UNLIMITED

**DTIC**  
**ELECTE**  
MAY 20 1980  
**S** **D**

**ROME AIR DEVELOPMENT CENTER**  
**Air Force Systems Command**  
**Griffiss Air Force Base, New York 13441**

80 5 19 020

DUPLICATE

This report has been reviewed by the RADC Public Affairs Office and is releasable to the National Technical Information Service. At NTIS it will be releasable to the general public, including foreign nations.

RADC-TR-80-24 has been reviewed and is approved for publication.

APPROVED:

*Joseph L. Horner*  
JOSEPH L. HORNER  
Project Engineer

APPROVED:

*Andrew C. Yang*  
ANDREW C. YANG, Chief  
Electro-Optical Device Technology Branch

APPROVED:

*Robert M. Barrett*  
ROBERT M. BARRETT, Director  
Solid State Sciences Division

FOR THE COMMANDER:

*John P. Huss*  
JOHN P. HUSS  
Acting Chief, Plans Office

If your address has changed or if you wish to be removed from the RADC mailing list, or if the addressee is no longer employed by your organization, please notify RADC (ESO) Hanscom AFB MA 01731. This will assist us in maintaining a current mailing list.

Do not return this copy. Retain or destroy.

UNCLASSIFIED

SECURITY CLASSIFICATION OF THIS PAGE (When Data Entered)

<b>REPORT DOCUMENTATION PAGE</b>		<b>READ INSTRUCTIONS BEFORE COMPLETING FORM</b>	
1. REPORT NUMBER <b>18</b> RADC-TR-80-24	2. GOVT ACCESSION NO. AD-A084349 <b>19</b>	3. RECIPIENT'S CATALOG NUMBER	
4. TITLE AND SUBTITLE <b>6</b> A STUDY OF REAL TIME SIGNAL PROCESSING METHODS FOR DECODING SPREAD SPECTRUM SYSTEMS.		5. TYPE OF REPORT & PERIOD COVERED Final Technical Report.	
6. PERFORMING ORG. REPORT NUMBER N/A		7. AUTHOR(s) <b>10</b> H. J. Caulfield Robert Haimes Peter Mueller	
8. PERFORMING ORGANIZATION NAME AND ADDRESS Aerodyne Research, Inc. Bedford Research Park, Crosby Drive Bedford MA 01730		9. CONTRACT OR GRANT NUMBER(s) <b>15</b> F19628-79-C-0032	
10. PROGRAM ELEMENT, PROJECT, TASK AREA & WORK UNIT NUMBERS <b>16</b> 62702F 46001928		11. REPORT DATE <b>17</b> February 1980	
11. CONTROLLING OFFICE NAME AND ADDRESS Deputy for Electronic Technology (RADC/ESO) Hanscom AFB MA 01731		12. NUMBER OF PAGES <b>11</b> 42	
14. MONITORING AGENCY NAME & ADDRESS (if different from Controlling Office) Same		15. SECURITY CLASS. (of this report) UNCLASSIFIED	
16. DISTRIBUTION STATEMENT (of this Report) Approved for public release; distribution unlimited.		15a. DECLASSIFICATION/DOWNGRADING SCHEDULE N/A	
17. DISTRIBUTION STATEMENT (of the abstract entered in Block 20, if different from Report) Same			
18. SUPPLEMENTARY NOTES RADC Project Engineer: Joseph L. Horner (RADC/ESO)			
19. KEY WORDS (Continue on reverse side if necessary and identify by block number) Spread Spectrum      Spectroscopy Optical Processing      Holography Matched Filtering      Time-Integrating Correlators Error Correcting Codes      Coherent Optics Acousto Optics      Optical Data Storage			
20. ABSTRACT (Continue on reverse side if necessary and identify by block number) Spread spectrum signals require several kinds of processing. First, the effects of tracking error, Doppler shifts, etc. must be compensated out or ignored in some clever way to give the "raw" signal. Second, the raw signal at high bandwidth must be decoded to give the low bandwidth information stream. Often this requires comparison of the raw signal with a properly-synchronized pseudo random reference signal. Third, the low bandwidth signal may or may not be burst error correction coded and			

390112

UNCLASSIFIED

SECURITY CLASSIFICATION OF THIS PAGE(When Data Entered)

Item 20 (Cont'd)

hence require appropriate decoding.

In this study we found that all three steps in spread spectrum decoding could be approached optically. Indeed, steps 1 and 2 can be so designed that a signal based in the visible or infrared can be processed "directly", i.e. so that the only detection occurs after both steps are done. Step 3 requires a reformatting of the bit stream (as all burst error correction methods must), but the optical realization is very fast and readily adaptable to error correcting codes of almost any form. This flexibility is because the optical decoding amounts to a look up table.

Specific, stand-alone developments from this program were two in number. First we developed a "generalized matched filter" which can be used just as a matched filter but which out performs the matched filter in several important ways. Second, we developed a way of obtaining a high spectral resolution tunable acoustooptic filter using existing components. Both developments should find wide application outside spread spectrum decoding.

UNCLASSIFIED

SECURITY CLASSIFICATION OF THIS PAGE(When Data Entered)

Evaluation

The report addresses some of the major problems in Spread Spectrum Communications Systems and discusses the role optical signal processing can play. The work focusses on the synchronization problems in acquiring the received code optically. This work was performed under TPO #R5D, "C<sup>3</sup> System Availability," the TPO Thrust being "Advanced C<sup>3</sup> Electronic Materials, and TPO Sub-Thrust," "Optical Signal Processing." The contract was in perfect harmony with all three of these.

*Joseph H. Horner*

JOSEPH H. HORNER  
Project Engineer

Accession For	
None	<input checked="" type="checkbox"/>
DD Form	<input type="checkbox"/>
Unprocessed	<input type="checkbox"/>
Processed	<input type="checkbox"/>
By _____	
Date _____	
Availability Code	
Dist	Availability Special
A	

TABLE OF CONTENTS

<u>Paragraph</u>	<u>Title</u>	<u>Page</u>
1	INTRODUCTION .....	5
1.1	Air Force Goals and Needs .....	5
1.2	Analysis Of Spread Spectrum Communication .....	5
1.3	Report Outline .....	6
2	OPTICAL DECODING METHODS .....	6
2.1	Operations Optics Can Perform .....	6
2.2	Synchronization With Long Codes .....	6
2.3	Direct Spectral Decoding .....	10
2.3.1	Overview .....	10
2.3.2	The Super High Resolution AOTF .....	12
2.3.3	Time Integrating Correlator .....	16
2.3.4	Generalized Matched Filters .....	16
2.4	Error Correcting Decoding .....	25
2.5	Conclusions Of The Decoding Study .....	26
3	A NEW SPREAD SPECTRUM METHOD .....	29
3.1	Introduction .....	29
3.2	Spatial Fourier Transformation .....	29
3.3	Spatial Filtering Of Spectral Fourier Transforms .....	31
3.4	Experimental Tests .....	33
3.5	Conclusions Of The New Method .....	33
4	CONCLUSIONS .....	37
	REFERENCES .....	38

LIST OF ILLUSTRATIONS

<u>Figure</u>	<u>Title</u>	<u>Page</u>
2.1	A Four-Day Code (a) Becomes A Cyclic Code (b) Which We Represent In 8 Overlapping One-Day Sections (c) .....	8
2.2	All Optical Spread Spectrum Decoder .....	11
2.3	For A Simple Grating At Wavelength We Require $d \sin \theta + d \sin \phi = n\lambda$ , Where $n = 0, \pm 1, \pm 2, \dots$ , Is The Diffraction Order .....	13
2.4	Gratings Of Spacings $d$ and $\delta$ Give An Equivalent Grating Of Spacing $\delta' = \left(\frac{1}{\delta} - \frac{1}{d}\right)^{-1}$ .....	15
2.5	Generalized Matched Filters For Distinguishing Between A Rectangle Function In White Noise And Just White Noise. The Generalized Matched Filter For The Rectangle Function Is A Matched Filter (A Sinc Function), While The Generalized Matched Filter For The Noise Is The Negative Of The Sinc Function .....	19
2.6	The GMF's For Two Rectangle Functions In White Noise And White Noise. Note That Sinc-Like Appearance Vanishes .....	21
2.7	A Pulse Train Containing Noisy Versions Of Three Equal- Energy Rectangle Function .....	22
2.8	The Response Of The Pulse Train Of Figure 2.7 Operated On By MF's For (a) The Highest (Narrowest) Rectangle, H (b) The Middle Height Rectangle, M, and (c) The Lowest (Widest) Rectangle L. Note The ambiguities, Especially With L. ....	23
2.9	The Response Of The Pulse Train Of Figure 2.7 to GMF's For (a) H, (b) M, And (c) L. Note The resolution Of All Amb- iguities As Well As The "Anticorrelations" At The Centers Of The "Wrong Pulses" .....	24
2.10	Desired Operations For Optical Error Correcting Decoding .....	27
2.11	Optical Arrangement For Error Correcting Decoding .....	28
3.1	Visibility Curves Corresponding To Various Spectral Distributions. Figure 7.54 Of Born & Wolf - <u>Principles</u> <u>Of Optics</u> .....	30
3.2	Functional Drawing Of The Laboratory System .....	34
3.3	Schematic Drawing Of The Laboratory System .....	35
3.4	The "White Light" Spectral Fourier Transform As Observed In The Spectral Filter Plane .....	36

## 1. INTRODUCTION

### 1.1 AIR FORCE GOALS AND NEEDS

The U.S. Air Force needs improved communications methods not only for increased bandwidth but also for increased security and margin against jamming, fading, multipath, and Doppler degradation. The purpose of this study was to determine which tasks in the receiver operations could best be done optically and to see how to do them. The particular communication method we studied in detail is spread spectrum communication (hereafter SSC) and, in particular, the most popular SSC method involving pseudo-random codes (PRC's) was emphasized.

There are many possible reasons for preferring optical signal processing to digital signal processing. They are seldom all simultaneously applicable. Such reasons include

- parallel processing,
- ability to handle very long codes,
- high bandwidth, and
- compatibility with optical storage methods.

We believed that optical processing would be most applicable in situations where the received signal is itself optical (in a broad sense) and noisy conversions of signal (and noise) from the optical domain to another (electrical or different-optical) domain could be avoided during the *first stages of the decoding process*. We called this "direct optical decoding".

### 1.2 ANALYSIS OF SPREAD SPECTRUM COMMUNICATION

The SSC technique utilizes a bandwidth  $B_t$  to transmit a message of bandwidth  $B_m$  and requires

$$B_t \gg B_m. \quad (1.1)$$

This spread in bandwidth (or "spectrum") offers error correcting possibilities. Let us call

$$R = B_t/B_m \quad (1.2)$$

the "spreading ratio". The PRC method starts with a string of  $R$ -bit\* code words which we can call  $W_1, W_2, \dots, W_N$ . With this string of code words we can send an  $N$ -bit message. We send  $1, 1, \dots, 1$  by sending  $W_1, W_2, \dots, W_N$ . We send  $0, 0, \dots, 0$  by sending  $W_1^c, W_2^c, \dots, W_N^c$ , where

$$W_k + W_k^c = 0 \quad (1.3)$$

---

\*These bits are sometimes called "chips," so "bit" can be used for our "word".

for  $k = 1, 2, \dots, N$ . Here the superscript  $c$  indicates the complement ( $1^c = -1, -1^c = 1$ ).

There are several possible decoding problems with the PRC version of SSC. First, synchronization to better than  $B_c^{-1}$  is required between the received signal and the code string being used for decoding. Even when synchronization is established, it is not automatically maintained because transmitter-receiver range, atmospheric effects, Doppler effects, etc. affect the arrival rate of signals. Some people have suggested that extremely long codes offer an extra layer of security in SSC. The time-bandwidth product for the total code word string is  $RN$ . Synchronization with a very large  $RN$  product might discourage enemy attempts to decode intercepted SSC signals. In addition even fairly short codes can offer considerable processing gain.

Second, even with synchronization, decoding may be difficult because of atmospheric effects (multipath, fading, etc.) and operating conditions (Doppler, poor tracking, etc.). These problems can be devastating in a system designed to be just sufficient in their absence. Of course, sufficient encoding (including burst error correction) can work in severe cases but the bandwidth suffers even more this way. Good system design is always a tradeoff.

### 1.3 REPORT OUTLINE

We deal primarily with decoding methods (Section 2) and secondarily with a new SSC method (Section 3). Thereafter, we seek to assess the impact of this program (Section 4).

## 2. OPTICAL DECODING METHODS

### 2.1 OPERATIONS OPTICS CAN PERFORM

We distinguish three possible tasks for optical decoding:

- 1 synchronization with long codes,
- 2 direct optical decoding of PRC signals, and
- 3 error correcting decoding.

### 2.2 SYNCHRONIZATION WITH LONG CODES

The basic concept, explored by other workers earlier (1), is to use the two-dimensional nature of the optical spatial filter correlator to correlate the received sequence with long codes. Two problems seem to appear. First, for codes of the length contemplated just storing the code on a single optical filter was beyond the state of the art. Second, there appears to be a bigger problem than just storing a record of the  $RN$  code bits properly. The problems which affect PRC decoding over the time of one code word affect it even more over  $N$  code words. Consider Doppler effects, for instance. These introduce subtle temporal scale changes in the received signal. Furthermore the Doppler effect is neither predictable nor stable. For which Doppler shift should the recognition search occur? It is clear that we must search both Doppler shifts and codes. The storage problem

becomes enormous.

Let us accept the hypothesis that we need to search only one (probably zero) Doppler shift and draw some conclusions and determine the feasibility from the storage-density point of view.

Horrigan and Stoner (1) have suggested optical correlation for code synchronization based on methods derived from Cohen and Moses (2). This has the advantage of using the two-dimensions available to optics in an optimum way. Even with two dimensions to work with, the total code length is so long as to be well beyond current technology.

Let us imagine a code of several days length. Periodically the sender transmits the message 1·1·1...1 (a synchronizing string). Our job is to locate that string of M bits in our stored record of P bits, where

$$P \gg M \gg 1. \quad (2.1)$$

We define

$B_t$  = base code transmission bandwidth, bits/sec.;

$T = M/B_t$  = duration of the synchronizing string, sec.;

$t = 1/B_t$  = duration of one bit or chip, sec.;

$\tau = P/B_t$  = duration of total code, sec.;

$D = \tau \times 1.157 \times 10^{-5}$  = duration of total code, days.

We assume we know what day of the code we are in. We divide the total code as shown in Figure 2.1. We should have no doubt as to which one-day-long segment it belongs to. In a one-day record there are

$$P_t = 8.64 \times 10^4 B_t$$

bits.

Our task is to utilize the methods already developed for optical processing and going beyond them to extend their applicability. Thus Horrigan and Stoner show that handling the very large  $P_t$  values required for one-day codes by spatial extension alone is impractical (see their Table 1).

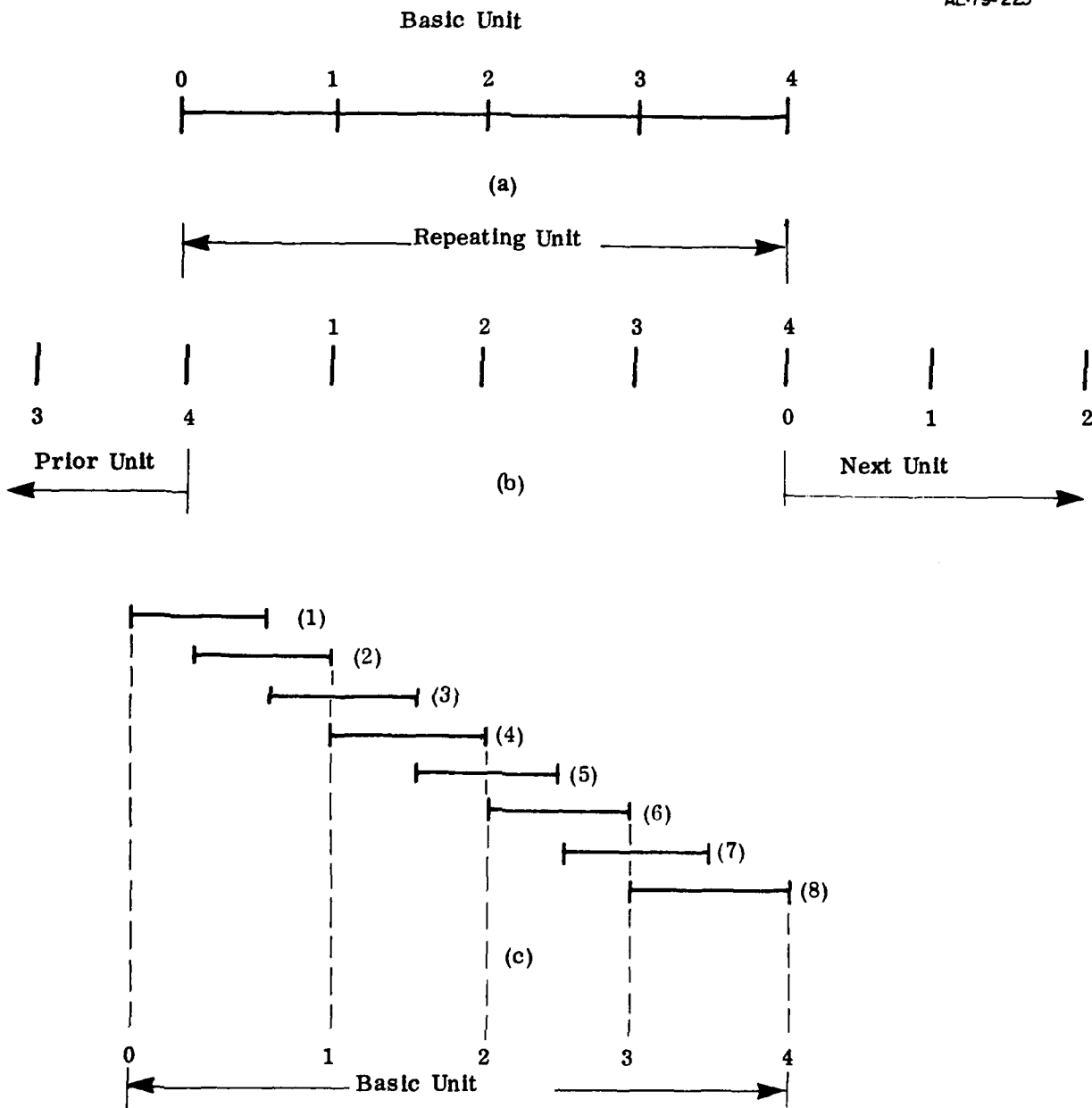


Figure 2.1 A four-day code (a) becomes a cyclic code (b) which we represent in 8 overlapping one-day sections (c)

If we assume that  $21.5 \text{ cm}^2$  ( $4.6 \text{ cm} \times 4.6 \text{ cm}$ ) is a reasonable mask size, we can handle 0.36 minutes at  $B_t = 10^8$ . This is a factor of 6000 off from the  $D = 1$  we want. The question then becomes: "How can we gain three orders of magnitude in storage without increasing the device size and complexity?" Were we to solve this problem, optics would offer an attractively compact and efficient vehicle for solving the synchronization problem.

There appears to be at least one way to accomplish this: use wavelength multiplexing. Castro et al (3) have developed a recording material which allows us to write over 1000 independent (orthogonal) spectral patterns into the same material. A reprint describing their method is attached. Using such a material we can

- (1) process the input against 1000 masks in parallel using incoherent optical methods and read out the detector plane in sequence using heterodyne detection or
- (2) process and read out one wavelength at a time using either coherent or incoherent methods.

As both processes require sequential readout and thus require the same time, we see no reason to do parallel processing of all spectral channels.

The question now is: "Do existing lasers give sufficient power to do this?" During  $T$  (assumed for the moment to be 0.36 minutes), we may want to process 1000 "frames" in separate spectral channels. We then have

$$T_F = T/1000 \quad (2.2)$$

as the time to interrogate each frame. For our example,  $T_F = 22 \text{ msec}$ . Following Horrigan and Stoner's example, we have

$$M = 2.147 \times 10^9.$$

Even if we use a CCD type detector array (none this size exist), we cannot interrogate at the rate  $B$  much less at  $MB$ . What we need is a way to reduce the electronic processing rate substantially. The only way we see to do this is to use an optical bistable device (4) to threshold out all but the correlation due to perfect synchronization. We would have

$$t_F = 0.36 \times 10^{-3} \text{ min.} = 19.6 \text{ msec}$$

to determine the  $x$ - $y$  location of that peak when it occurs. Centroid detectors with greater than  $\sqrt{M}$  = resolvable units in each direction are available commercially (5). These are silicon detectors, so we can assume a good quantum efficiency,  $\eta$ . We will assume, pessimistically,  $\eta = 0.1$ . To locate to one part in  $\sqrt{M}$ , we want at least

$$N_p = 100 M$$

photons. Assume a wavelength  $\lambda$ , and a laser power  $P_L$ , then we want

$$\left( \frac{\eta P_L \lambda}{hc} \right) t_F \geq 100 \text{ M.}$$

where h is Planck's constant and c is the speed of light. For  $\lambda = 0.5 \mu\text{m}$  (green light), we need (for this example)

$$P_L > \frac{100 \times 2.147 \times 10^9 \times 6.626 \times 10^{-34} \times 3 \times 10^8}{0.1 \times 0.5 \times 10^{-6} \times 1.96 \times 10^{-2}}$$

$$= 43.5 \mu\text{w.}$$

This level is easily obtained with every commercially available tunable dye laser. The frequency tuning rate must be faster than 20 msec per wavelength. One milli-second times are not unreasonable for a stepping motor to rotate a prism to change the wavelength.

It thus appears that the combination of processing techniques already devised with some of the newest optical devices (wavelength hole burning, bistable devices, and centroid locators) can handle the full synchronization problem. This system is very compact and can perform correlations over the whole one-day code during a time equal to that required to accumulate M bits, so all bits can be tested on line.

A far more modest task can be valuable as well. Most digital electronic correlators can handle no more than about 1000 bits, while optics can handle 10,000 or more rather easily. Decoding "short" codes may represent a useful application of optics.

## 2.3 DIRECT SPECTRAL DECODING

### 2.3.1 Overview

We have reached here the key part of our effort. The idea is to postpone optical-to-electrical conversion until after PRC decoding (with various sources of noise and jamming filtered out optically and Doppler, synchronization, fading, and pointing errors continually counteracted optically). Thus the detector sees only the noise-filtered message at bandwidth  $B_m$ . Large gains in jam immunity and in signal-to-noise ratio may be expected if such a task can be accomplished.

A question naturally arises as to what wavelength limitations exist in this method. We shall see that the limitations are largely on materials in the components and, in particular, in acousto-optic materials which we know to work from  $0.3 \mu\text{m}$  to  $11 \mu\text{m}$ . We have no data on longer wavelengths, so the ultimate long wavelength limits are unknown.

Figure 2.2 shows the major system components. A standard tracking telescope keeps the centroid of the signal through the narrow band\* filter. This beam is then spectrally filtered by a new acousto optic tunable filter (AOTF's) invented

\* Wide enough to encompass all reasonable Doppler shifts.



under this contract to achieve a narrower spectral band pass than prior AOTF's and to track Doppler shifts. The beam so tracked and filtered passes through a time integrating correlator (TIC) to a detector array which allows synchronization tracking. Fading (measured after spectral filtering) and Doppler shifting (measured by the correction needed to maintain the proper location of the spectrally filtered signal) are taken into account in the amplitude and time scale of the signal fed to the TIC.

Finally, the signal correlated against is not a section of the code word string  $W_1, W_2, \dots, W_N$  but a modified version far more tolerant of Doppler, etc. This modified correlation, which we call "generalized matched filtering" (GMF) is certainly the most widely-applicable invention of this work.

### 2.3.2 The Super High Resolution AOTF

Here we discuss the AOTF system invented under this contract. We believe it is widely applicable. AOTF's have become valuable tools in modern electrooptic systems (6). This invention is a new way to use them.

In their simplest form, AOTF's are simply variable-spacing gratings. In fact they are thick holographic gratings, so their Bragg diffraction efficiency can be quite high (7). One difficulty with AOTF's has been that their resolving power is still rather modest. We show here a rather simple way to increase their resolving power significantly at a concomitant price of reducing the tunability range. Indeed the number of spectral channels is conserved but their width is now controllable

The basic idea is to achieve the high dispersion with a nontunable element, e.g. a grating. The tuning is done by changing the angle of incidence of light on the fixed disperser with an AOTF. Together, the AOTF and the fixed disperser comprise a system equivalent to a single highly-dispersive grating with limited tunability.

In the analysis which follows we use simple, thin-grating equations for simplicity. Figure 2.3 shows a simple grating of length  $L$  and spacing  $d$  diffracting light of wavelength  $\lambda$  from an incident angle  $\theta$  to an exit angle  $\phi$ . For constructive interference we require

$$d \sin \theta + d \sin \phi = n\lambda, \quad (2.4)$$

where  $n$  is an integer (the diffraction order). In other words

$$\sin \phi = \frac{n\lambda}{d} - \sin \theta. \quad (2.5)$$

Diffraction limits the resolution to

$$\Delta \sin \phi \sim \frac{\lambda}{L}. \quad (2.6)$$

The effect of dispersion is

$$\Delta \sin \phi = \frac{n\Delta\lambda}{d}. \quad (2.7)$$

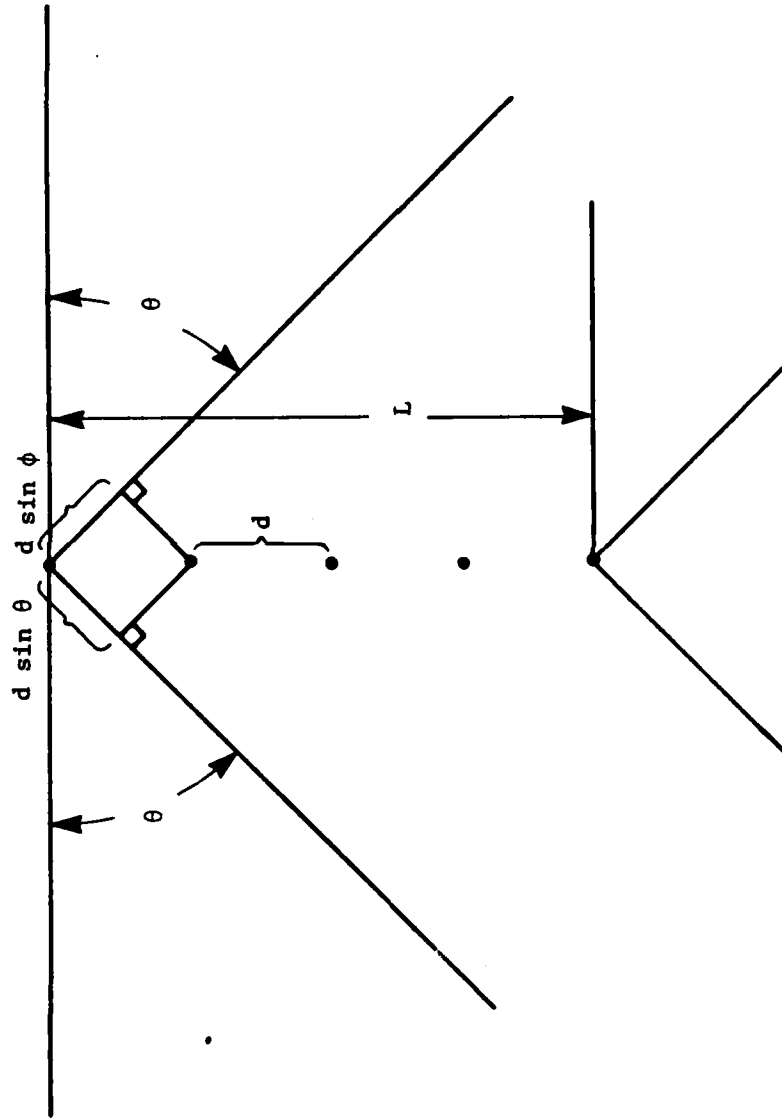


Figure 2.3 For a simple grating at wavelength  $\lambda$  we require  $d \sin \theta + d \sin \phi = n\lambda$ , where  $n = 0, \pm 1, \pm 2, \dots$  is the diffraction order.

Thus the diffraction-limited resolving power is

$$R \triangleq \frac{\lambda}{\Delta\lambda} = n \left( \frac{L}{d} \right) = n N_o, \quad (2.8)$$

where

$$N_o = L/d \quad (2.9)$$

is the number of lines in the grating. Figure 2.4 shows two gratings of length  $L$  cascaded. If the grating spacing of the first grating is  $d$  and the grating spacing of the second grating is  $\delta$ , it is easy to see that the output angle  $\psi$  is given by

$$\sin \psi = \frac{n\lambda}{\delta'} + \sin \theta. \quad (2.10)$$

Here

$$\frac{1}{\delta'} = \frac{1}{\delta} - \frac{1}{d}. \quad (2.11)$$

Calling  $\psi(\lambda, \delta')$  the angle we would observe for wavelength  $\lambda$  if  $\delta = \delta'$ , we have

$$\sin \psi(\lambda, \delta') = \sin \psi(\lambda, \delta) - \frac{n\lambda}{d}. \quad (2.12)$$

We can tune  $d$  over

$$L/N_o \leq d \leq L. \quad (2.13)$$

This swings  $\sin \psi(\lambda, \delta')$  over

$$\frac{n\lambda}{L} \leq \sin \psi(\lambda, \delta) - \sin \psi(\lambda, \delta') \leq \frac{n N_o \lambda}{L} \quad (2.14)$$

Dispersion gives

$$\Delta \sin(\lambda, \delta') \approx \Delta \sin(\lambda, \delta) = \frac{n \Delta \lambda}{\delta}. \quad (2.15)$$

so the wavelength tuning range is

$$\Delta \lambda \approx \left( \frac{\delta}{d} \right) \lambda. \quad (2.16)$$

For practical cases we might have  $d/\delta \sim 100$ , so we can get a factor of 100 increase in resolution at the price of a factor of 100 decrease in the tuning range.

It is obvious that such an AOTF system could be very useful in decoding a frequency hopping system with only one channel rather than one channel per frequency.

AL-79-442

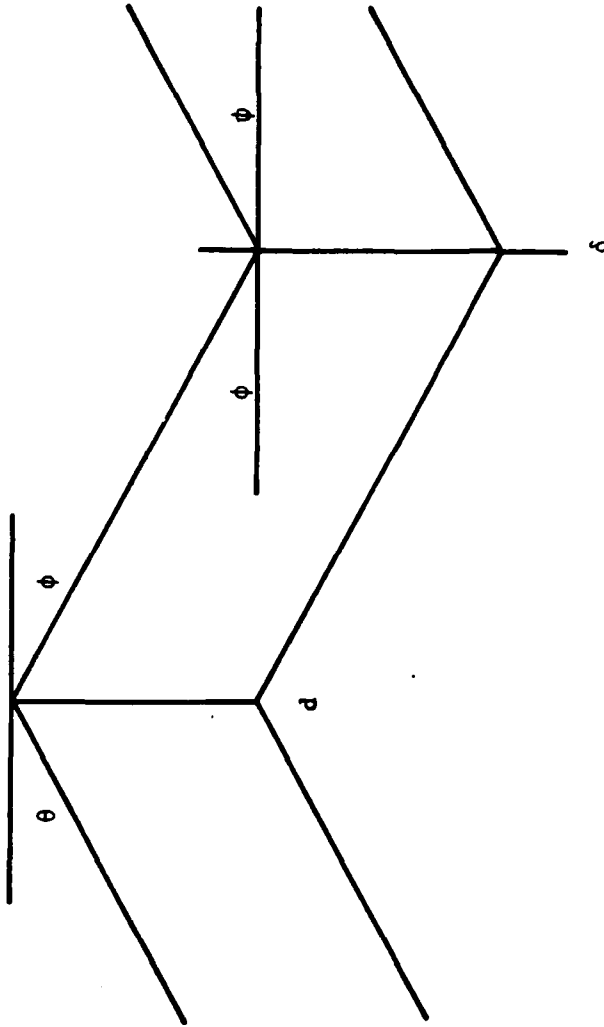


Figure 2.4 Gratings of spacings  $d$  and  $\delta$  give an equivalent grating of

$$\text{spacing } \delta' = \left( \frac{1}{\delta} - \frac{1}{d} \right)^{-1}$$

Using this new AOTF system we seek to keep the maximum signal on axis. From the tuning required to do so we track Doppler shifts. We integrate over a time of about  $N/B_t$  to assure a sample independent of the exact form of  $W_k$ .

### 2.3.3 Time Integrating Correlator

The "classical" TIC (8) (9) contemplates modulating a laser beam to create a time signal  $S_1(t)$ , superimposing  $S_1(t)$  at all points along an acousto-optic modulator (x direction along its axis), sending the signal  $S_2(t - \frac{x}{v})$  across the modulator at speed  $v$ , imaging the modulator onto a detector array, and time integrating. The output signal at  $x$  is

$$O(x, \tau_1, \tau_2) = \int_{\tau_1}^{\tau_2} S_1(t) S_2(t - \frac{x}{v}) dt, \quad (2.17)$$

which we recognize as a cross correlation function if  $S_1$  and  $S_2$  are real.

In our case we already have a modulated, monochromatic light beam, so all we need to do is impact it on an acousto-optic modulator driven by  $S_2(t)$  and image onto the detector array. We should obtain the peak signal (integrated over a time of  $N/B_t$ ) at the center of the array for perfect synchronization. Now we can track synchronization continuously with a time constant of  $N/B_t$ .

### 2.3.4 Generalized Matched Filters

Here we reach what we believe to be the most important invention resulting from this work. In the following description we cast the GMF in terms of its two-dimensional aspect as well as its one-dimensional aspect. We conclude that wherever matched filters are useful, generalized matched filters are probably more useful.

Matched filtering has become the primary tool of optical pattern recognition despite the fact that matched filters fail to take into account either the differences among patterns of classes we wish to distinguish or differences among patterns belonging to the same class. Thus a filter matched to the letter "A" is the same whether or not we wish to tolerate rotations, scale changes, or other distortions and, of course, independently of the magnitudes or probabilities of those distortions. Likewise the filter matched to the letter "A" is the same regardless of what we are trying to distinguish it from, e.g. "B", "C" or "B" and "C". For many years we have sought a way to adapt filters to the specific job. Caulfield and Maloney (10) showed that filters matched to linear combinations of the undistorted "character alphabet" could be made to give maximum distinguishability between undistorted input patterns. They also showed that these new filters were somewhat more tolerant to input distortions than were matched filters. What we describe here is a fully general solution to the problem of generating the optimum filter (which of course, may not be the matched filter) for each particular problem. We call these new filters "generalized matched filters" or GMF's because they reduce to the matched filters (MF's) when the problem is the simple one for which MF's are known to be optimum. For all more complicated cases the GMF's will be superior to MF's in both insensitivity to distortions we want to tolerate and sensitivity to between-class differences.

While the GMF is, to our knowledge, a new concept, the mathematical tools upon which it is based are very old. The new contribution described here is that of formulating the GMF problem in such a way that it is clear that the prior mathematical methods describe it.

Let us describe digital matched filtering. A discrete-point input function  $f(x_m, y_n)$  is Fourier transformed to produce a discrete-position Fourier transform  $F(u_k, v_l)$ . Then  $F(u_k, v_l)$  is multiplied by the matched filter  $M(u_k, v_l)$ , that product is retransformed, and the resulting pattern  $g(\xi_p, \eta_q)$  is examined. If the centroid of  $f(x_m, y_n)$  is at  $x_m = 0, y_n = 0$ ; then we want to evaluate  $f(0, 0)$  is simply

$$g(0, 0) = \sum_k \sum_l F(u_k, v_l) M(u_k, v_l). \quad (2.18)$$

Formulated in this way, the problem of deriving the filter  $M(u_k, v_l)$  can be recognized as a special case of "linear discriminant analysis" (11) which, in turn, is a special case of "principal component analysis" (12). Rather than repeat the known mathematics in detail here, we simply describe what linear discriminant functions (LDF's) are and in what sense they are optimum. We suppose that  $N$  measurements are made on each input object and call those measurements for the unknown object  $x$  the measurement vector  $\vec{x} = (x_1, x_2, \dots, x_N)$ . Let there be  $K$  classes of objects ( $C_1, \dots, C_K$ ) and  $K$  linear discriminant functions ( $LDF_1, \dots, LDF_K$ ). The operation

$$LDF_1(\vec{x}) = S_1(\vec{x}) \quad (2.19)$$

gives a real number  $S_1(\vec{x})$ . Indeed

$$LDF_1(\vec{x}) = \vec{V}_1 \cdot \vec{x} + S_{01}, \quad (2.20)$$

where

$$\vec{V}_1 = (V_1, \dots, V_N) \quad (2.21)$$

is a set of real numbers and  $S_{01}$  is a real number.

The LDF's are so chosen that

$$[LDF_1(\vec{x} \in C_i) - LDF_1(\vec{x} \notin C_i)] \quad (2.22)$$

is maximum, where  $\mathcal{E}[\cdot]$  is the expected value operator.  $LDF_1$  is that linear combination of  $x_n$ 's most likely to distinguish between  $\vec{x} \in C_1$  and  $\vec{x} \notin C_1$ . Usually the LDF's are normalized so that

$$\mathcal{E} \left[ LDF_1(\vec{x} \in C_j) \right] = \delta_{ij} \quad (2.23)$$

Thus, for an unknown  $\bar{x}$ , we evaluate all of the  $S_1(\bar{x})$ 's. If the maximum one is  $S_k(\bar{x})$ , we assign

$$\bar{x} \in C_k. \quad (2.24)$$

The optimization is designed to give a minimum expected error using such a decision algorithm.

Our approach is to make the feature vector for  $f(x_m, y_n)$  the set of  $\{F(u_k, v_l)\}$  ordered in any arbitrary way. The LDF's give a "filter"  $V(u_k, v_l)$ . The  $S_{0,1}$ 's give thresholds.

Let us now look at some GMF's. If we expect no distortions of  $f(s, y)$  and no other images in the field, then we can write

$$C_1 = \{f(x, y) + n(x, y)\} \quad (2.25)$$

and

$$C_2 = \{n(x, y)\} \quad (2.26)$$

where  $\{n(x, y)\}$  represents the noise

For this case we would expect

$$LDF_1 = MF_1 \quad (2.27)$$

and, if  $\mathcal{E}[n(x, y)] = n_0$ ,

$$LDF_2 = -MF_1 \quad (2.28)$$

That is, to recognize noise ( $C_2$ ) we say "noise is what is not signal". For simplicity we chose

$$C_1 = \{\text{rect}(x) + n(x)\} \quad (2.29)$$

and

$$C_2 = \{n(x)\} \quad (2.30)$$

where

$$\mathcal{E}[n(x)] = 0.1. \quad (2.31)$$

Figure 2.5 shows the two GMF's. We recognize

$$GMF_1 = MF_1 = \text{sinc}(u) \quad (2.32)$$

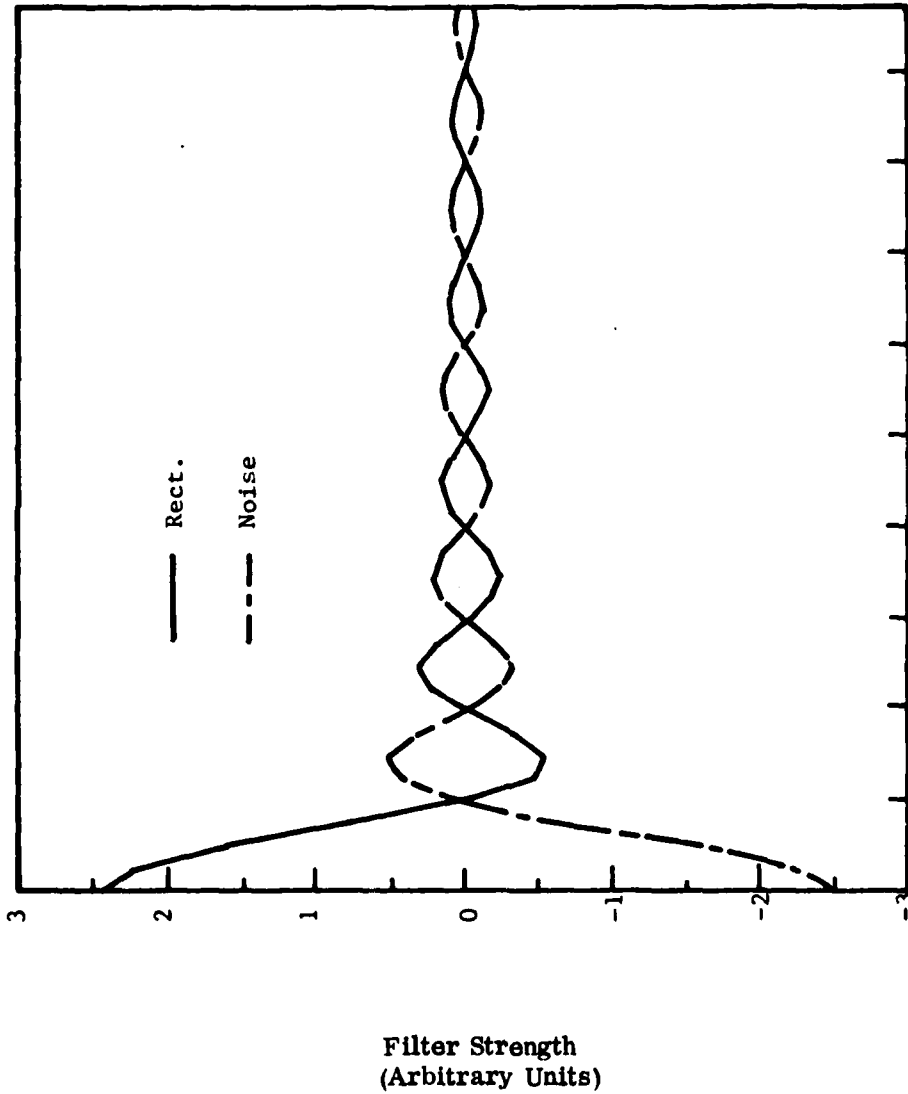


Figure 2.5 Generalized matched filters for distinguishing between a rectangle function in white noise and just white noise. The generalized matched filter for the rectangle function is a matched filter (a sinc function), while the generalized matched filter for the noise is the negative of the sinc function.

and

$$\text{GMF}_2 = \text{MF}_2 = -\text{sinc}(u) \quad (2.33)$$

Thus the MF is a special case of the GMF

Now if we have

$$C_1 = \{ \text{rect}(x) + n(x) \} \quad (2.34)$$

$$C_2 = \{ \text{rect}(2x) + n(x) \}, \text{ and} \quad (2.35)$$

$$C_3 = \{ n(x, y) \}, \quad (2.36)$$

we have no expectation other than that the GMF's should not be the MF's. Figure 2.6 shows the resulting GMF's.

To test performance of the GMF's we went to an even harder problem:

$$C_1 = \left\{ \frac{1}{6} \text{rect}(6x) + n(x) \right\}, \quad (2.37)$$

$$C_2 = \left\{ \frac{1}{7} \text{rect}(7x) + n(x) \right\}, \quad (2.38)$$

$$C_3 = \left\{ \frac{1}{8} \text{rect}(8x) + n(x) \right\}, \quad (2.39)$$

$$C_4 = n(x). \quad (2.40)$$

We placed samples of these noisy, equal-energy rectangle functions in a series as shown in Figure 2.7. Operation on this series with the first three MF's Figure 2.8 gave poor discrimination. Operating on the same series with the first three GMF's Figure 2.9 gave excellent discrimination. Measuring at the centers [g(0,0) of our previous analysis] we obtained the following response matrices (normalized to unity diagonal elements):

		MF RESPONSES		
		1	2	3
I N P U T S	1	1	0.96	0.92
	2	0.81	1	1
	3	0.64	0.82	1

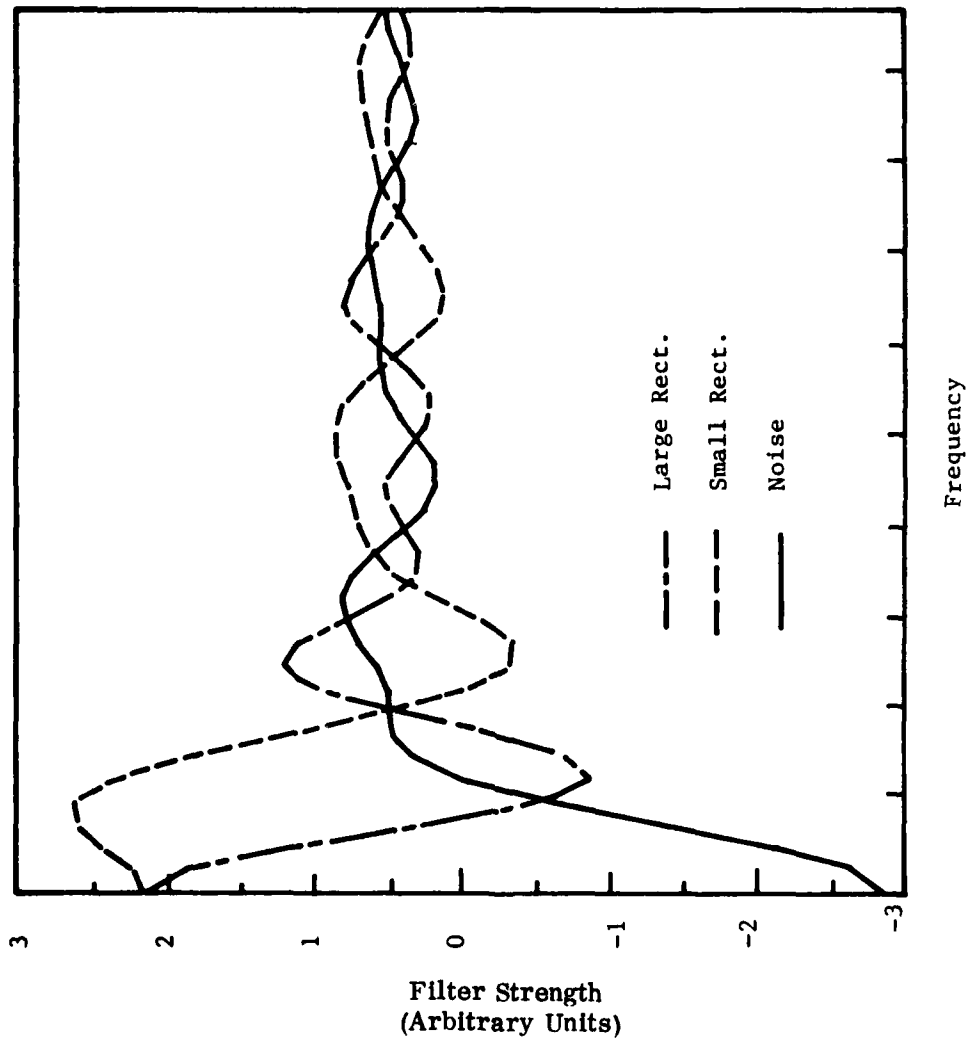
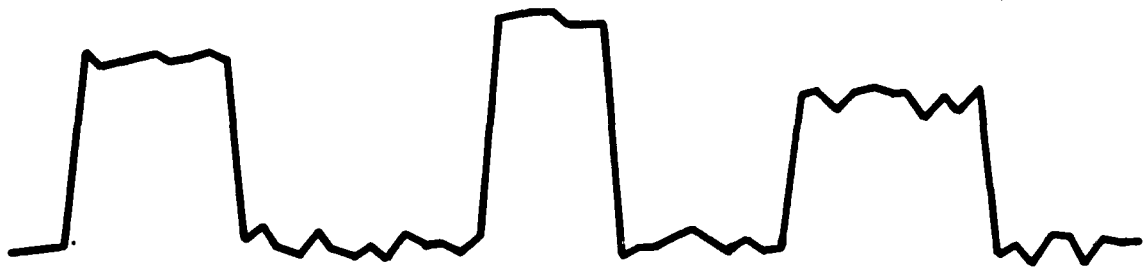
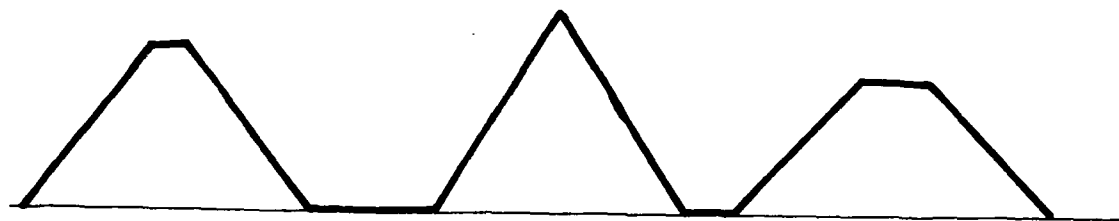


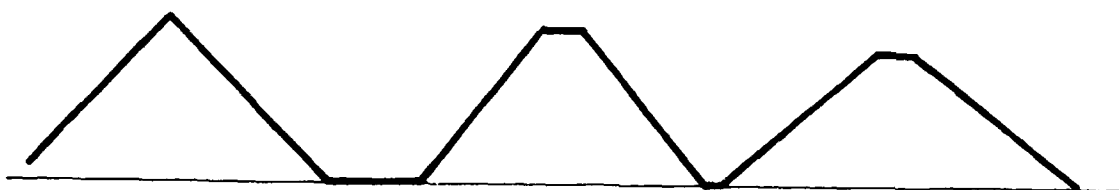
Figure 2.6 The GMF's for two rectangle functions in white noise and white noise. Note that sinc-like appearance vanishes.



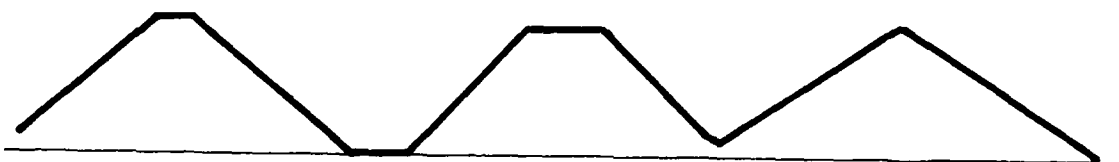
**Figure 2.7** A pulse train containing noisy versions of three equal-energy rectangle function.



(a)

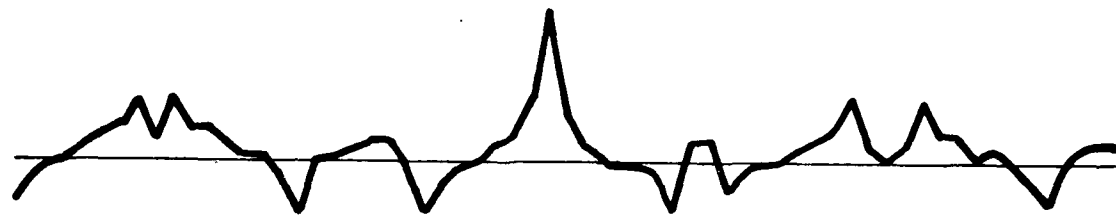


(b)

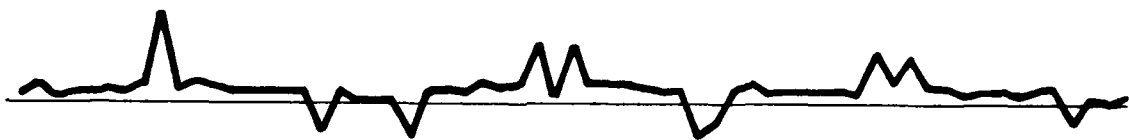


(c)

Figure 2.8 The response of the pulse train of Figure 2.7 operated on by MF's for (a) the highest (narrowest) rectangle. H (b) the middle height rectangle, M, and (c) the lowest (widest) rectangle L. Note the ambiguities, especially with L.



(a)



(b)



(c)

Figure 2.9 The response of the pulse train of Figure 2.7 to GMF's for (a) H, (b) M, and (c) L. Note the resolution of all ambiguities as well as the "anticorrelations" at the centers of the "wrong pulses".

### GMF RESPONSE

		1	2	3
I N P U T S	1	1	0.07	- 0.28
	2	0.38	1	- 0.04
	3	0	- 0.66	1

The average value of the difference between on-axis and off-axis elements is only 0.14 for MF's (poor discrimination) but is 1.10 for GMF's (good discrimination) when the on-axis terms are equal. Another comparison is worst cases. The worst case differences for MF's is 0.00. The worst case difference for GMF's is 0.62.

While many practical problems with optical implementation of GMF's are obvious (separating real and imaginary parts, digital filter generation, handling large numbers of GMF sample points, etc.), the basic conclusions are clear. Matched filtering is a special case of the far more general and powerful technique which we call generalized matched filtering.

#### 2.4 ERROR CORRECTING DECODING

While the method we describe is both simple and promising, its explanation can be confusing. Careful definition of the problem is essential. We receive MN message bits, where M and N are preassigned integers. The bits arrive serially and can be called  $b_1, b_2, \dots, b_{MN}$ . If we have a burst error correcting code, we must rearrange the received bits before decoding. Typically, we might arrange them into N groups of M bits each something like:

$$\begin{array}{cccc}
 b_1 & b_{N+1} & \dots & b_{NM+1-N} \\
 b_2 & b_{N+2} & \dots & \dots \\
 \dots & \dots & \dots & \dots \\
 \dots & \dots & \dots & \dots \\
 b_N & b_{2N} & \dots & b_{NM}
 \end{array}$$

Thus a burst error of up to N bits can affect at most one bit in each of the N words (rows). Now if we can correct for a few (much less than M) bit errors in a word, we have achieved a large degree of immunity to burst errors. To correct for up to P bit errors, we restrict the transmitted message to being words from the set of codes  $\{CW_1, CW_2, \dots, CW_Q\}$  which have the property that for  $i \neq j$ ,  $CW_i$  and

$CW_k$  differ in at least  $2P+1$  places (the "Hamming distance" is at least  $2P+1$ ). Identifying each row of the matrix just formed (e.g. row 1 comprising  $b_1, \dots, b_{NM+1-N}$ ) as a received word  $RW_k$  ( $RW_1$  in this example), we want to find the Hamming distance between  $RW_k$  and each of the  $Q$  code words. The closest code word is assumed to be the message word. Clearly  $P$  bit errors can be corrected in this way.

We now recognize that if we encode 1's and 0's as spatially-complementary patterns, e.g.



then template matching (or, equivalently, matched filtering) of the received word with each code word will give signals whose differences are proportional to the Hamming distances between the received word and each of the code words.\* Thus matched filtering can be used for error correcting decoding.

The required process is shown in Figure 2.10, while Figure 2.11 shows the system layout. In Figure 2.10, we show five steps. Steps 3 and 4 can be done optically as shown in Figure 2.11. Each received word is arranged on one line in the  $x$  direction. A total of  $N$  received words can be handled in parallel. A cylindrical lens Fourier transforms  $X$  into  $U$  and allows spreading in the  $V$  direction. The holographic mask has  $Q$  multiplexed words encoded on it, each at a distinct angle and all in the  $U$  direction. There is no  $V$  variation. A second cylindrical-spherical lens Fourier transforms the  $U$  direction into  $\xi$  and images  $V$  into  $\eta$ . Along the output  $\xi$  row corresponding to the input  $x$  rows of code word  $n$ , we find  $Q$  correlation spots (one for each of the error correcting code words. The  $\xi$  value corresponding to the strongest correlation gives the error corrected message of word  $n$ .

Optical decoding has two great advantages over electronic decoding - speed (from parallel operations) and versatility (all codes are equally easy to handle).

## 2.5 CONCLUSIONS OF THE DECODING STUDY

It is now clear that spread spectrum signal decoding by optical means is practical and useful for

- . synchronizing with longer-than-1000-bit codes (if the code lengths are not so long as to preclude synchronization altogether).
- . correlating in a way designed to take statistically-predictable distortions into account, and
- . decoding burst-error-correcting codes.

The direct optical decoding of pseudo-randomly coded spread spectrum radiation (so that the detectors see only the decoded message bits) is both feasible and worthwhile.

\*This follows directly from the template-matching interpretation of matched filtering.

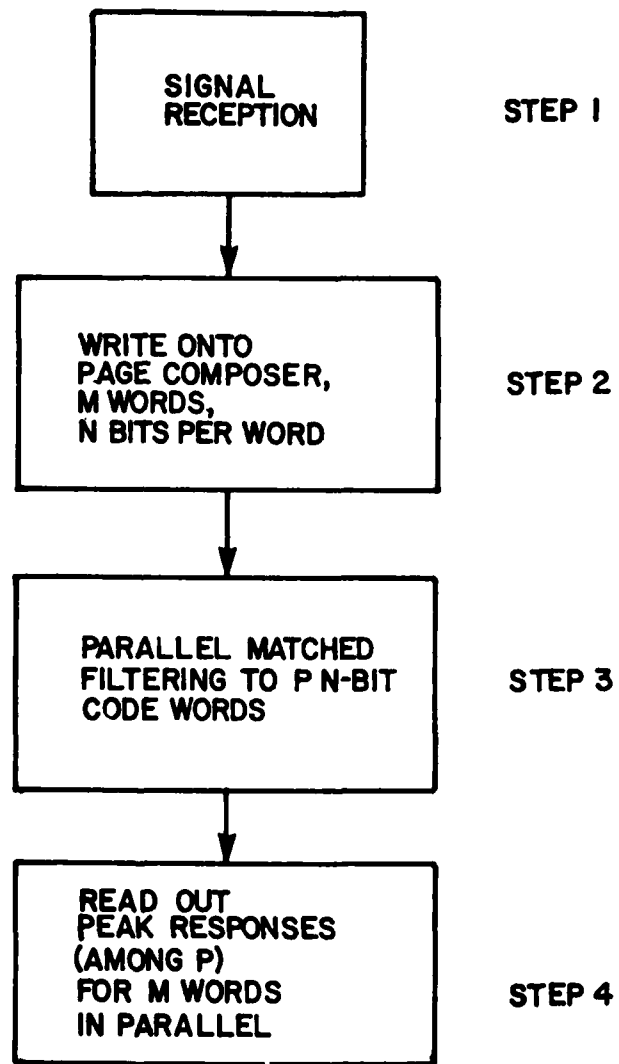


Figure 2.10 Desired Operations For Optical Error Correcting Decoding

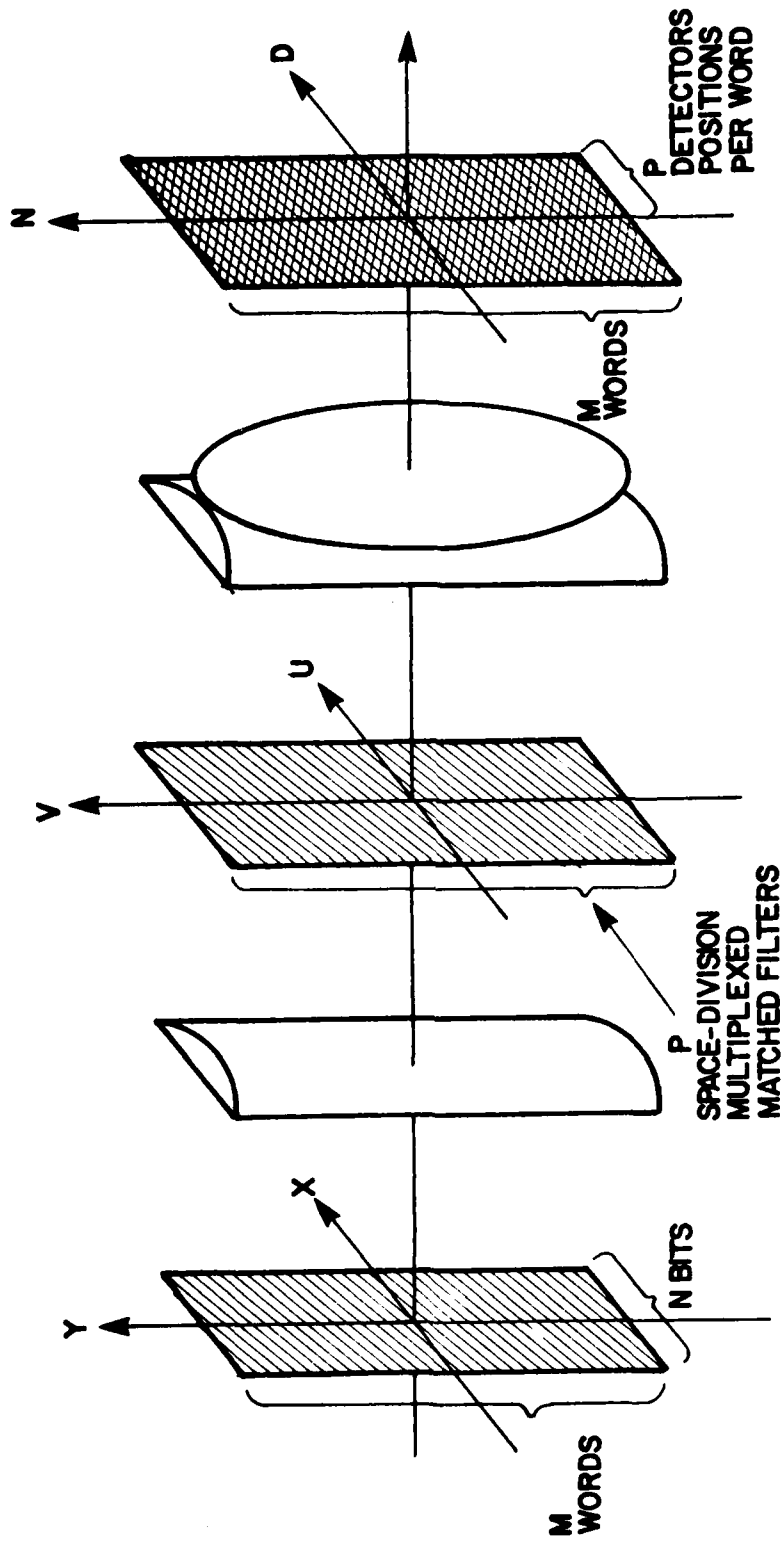


Figure 2.11 Optical Arrangement For Error Correcting Decoding

### 3. A NEW SPREAD SPECTRUM METHOD

#### 3.1 INTRODUCTION

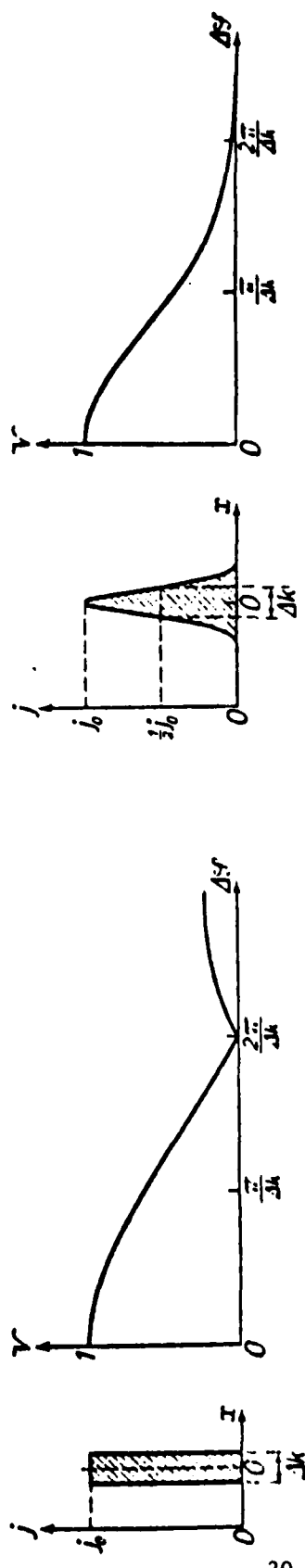
The basic idea here is to use polychromatic radiation which is spectrally encoded. One such method is called "frequency hopping". In frequency hopping, successive message bits are sent over discrete, non-overlapping spectral channels. Thus the bandwidth for the message exceeded that for any bit. Our approach was to use the full bandwidth for each bit. The way to do this while still utilizing spectral encoding is to utilize different spectral weightings for different "channels". For example, we might operate on the Fourier transform of the source spectrum in such a way that the various "channels" are separable only in Fourier transformation.

#### 3.2 SPATIAL FOURIER TRANSFORMATION

Here we want to show how a spatial display of the cosine Fourier transform of the source spectrum can be obtained by interferometry. The basic insight is due to Michelson and is covered well by Born and Wolf (13). Modern interferometers to accomplish this are reviewed by Caulfield (14, 15, 16). The basic idea is that an interferometric fringe pattern is simply the spatial display of modulo  $\lambda$  ( $\lambda$  being the wavelength) equal-paths from the source. If the path difference is a linear function of position in the fringe field (as when the fringes are formed by two mutually-inclined collimated beams), the envelope of the interference pattern is the cosine Fourier transform of the spectral source distribution. Figure 3.1 shows an example from Born and Wolf (13) who plot the envelope or fringe visibility as a function of source bandwidth in wavenumber (which they call  $\Delta k$ ) and path difference (which they call  $\Delta \varphi$ ).

Consider an interferometer which splits the light into two collimated beams and interferes them at an angle. Let  $x$  be the dimension normal to the bisector of the angle between the two beams and in the plane of that angle. Call  $x = 0$  the position of perfect path matching. At all other points ( $x \neq 0$ ) the wavefront for one beam passes  $x$  before the wavefront from the other has arrived. The time difference is proportional to  $x$ . Thus we have a linear spatial display of relative time differences between the rays travelling the two paths. The power between wavenumbers  $\sigma$  and  $\sigma + d\sigma$  is  $S(\sigma)d\sigma$ . The amplitude of that light varies as the cosine of the frequency  $\nu = c\sigma$  times the relative time delay (proportional to  $x$ ). The sum (integral) of  $S(\sigma)$  over all  $\sigma$ 's is simply the cosine Fourier transform of  $S(\sigma)$ .

In earlier applications (14) this spatial pattern was used as a means for deducing  $S(\sigma)$  rather than measuring it directly with a dispersive spectrometer. Because no scanning occurs, arbitrarily short pulses can be handled in this way. Because all wavenumbers contribute at every point, some dynamic range problems are obviated. The application we will describe here is totally new. This is the first study devoted to spectral modulation in such an interferometer.



(a)

$= j_0$  when  $|x| < \frac{1}{2}\Delta k$ ,  
 $= 0$  when  $|x| > \frac{1}{2}\Delta k$ ,

$$V = \frac{|\sin(\frac{1}{2}\Delta k \Delta S)|}{|\frac{1}{2}\Delta k \Delta S|}$$

(b)

$$= j_0 e^{-\alpha^2 x^2},$$

$$V \sim e^{-\left(\frac{\Delta S}{2\alpha}\right)^2}.$$

Figure 3.1 Visibility curves corresponding to various spectral distributions  
 Figure 7.54 of Born & Wolf - Principles of Optics

### 3.3 SPATIAL FILTERING OF SPECTRAL FOURIER TRANSFORMS

Let us consider two modified Mach-Zehnder interferometers in series which have compensating effects. That is all paths through the two are of equal length, but there is an intermediate plane where the cosine Fourier transform appears. Suppose that the source spectrum is  $S(\sigma)$ . Then the spatial cosine Fourier transform is

$$s(x) = \int_0^{\infty} S(\sigma) \left[ 1 + \cos(2\pi\sigma x \cos\theta) \right] d\sigma, \quad (3.1)$$

where  $\sigma$  is the wavenumber and  $S(\sigma)d\sigma$  is the power between  $\sigma$  and  $\sigma+d\sigma$ . But we bound the  $x$  plane between  $x_1$  and  $x_2$ , so the output spectrum is (except for irrelevant multiplicative factors)

$$S_o(\sigma) = \int_{x_1}^{x_2} s(x) \left[ 1 + \cos(2\pi\sigma x \cos\theta) \right] dx. \quad (3.2)$$

If we insert a mask  $M(x)$  in the Fourier transform plane we obtain an output spectrum

$$S_m(\sigma) = \int_{x_1}^{x_2} s(x) m(x) \left[ 1 + \cos(2\pi\sigma x \cos\theta) \right] dx. \quad (3.3)$$

The cosine Fourier transform of that spectrum is

$$s_m(x) = \int_{\sigma=0}^{\infty} S_m(\sigma) \left[ 1 + \cos(2\pi\sigma x \cos\theta) \right] d\sigma. \quad (3.4)$$

The display  $s_m(x)$  is the result of insertion of the mask  $m(x)$ . It was our initial hope that we would find

$$s_m(x) = B + m(x), \quad (3.5)$$

where  $B$  is a background term. In retrospect that hope can be seen to be naive. The best example of the proper approach is the Selective Interferometric Modulation System (SIMS) which is a special case of our method (17). In SIMS we set

$$m(x) = 1 + \cos(2\pi\sigma_0 x \cos\theta). \quad (3.6)$$

Note that the peaks of  $m(x)$  hit where the peaks of  $1 + \cos(2\pi\sigma_0 x \cos\theta)$  are.

The effect is to transmit light of wavenumber  $\sigma_0$  preferentially. Then they move to

$$m(x) = 1 + \sin(2\pi\sigma_0 x \cos\theta) \quad (3.7)$$

which attenuates  $\sigma_0$  selectively. Thus SIMS can modulate one wave number component of the spectrum. We must modulate in a well-defined, distributed filter function. The mask which leads to a peak at

$$x = 1/\sigma_0 \cos\theta \quad (3.8)$$

is, of course,

$$m(x) = 1 + \cos(2\pi\sigma_0 x \sin\theta). \quad (3.9)$$

Thus it is clear that  $s_m(x)$  and  $m(x)$  are not similar in shape. Furthermore the example we chose [ $s_m(x)$  with a local peak at  $x = 1/\sigma_0 \cos\theta$ ] is easily detectable with a spectrometer tuned to  $\sigma = \sigma_0$ . A communication system based on this is no more secure than a system based on a prism or grating spectrometer. What we need is to choose a more complicated  $x$  pattern we want to detect. Call it  $p(x)$ . Then we set

$$m(x) = \frac{p(x)}{s(x) + C} \quad (3.10)$$

where  $C$  is a small constant used to avoid singularities.

Now it is clear that we can choose  $N$  orthogonal patterns  $p_1(x), p_2(x), \dots, p_N(x)$ . That is

$$\int_{x_1}^{x_2} p_i(x) p_j(x) dx = \delta_{ij}. \quad (3.11)$$

The corresponding masks are  $m_1(x), m_2(x), \dots, m_N(x)$ . We can use  $N$  independent channels separated in the direction normal to the beam splitting plane. By modulating the  $k^{\text{th}}$  channel and observing through the corresponding mask  $p_k(x)$  in the spatial Fourier transform of the receiver, we can communicate over the  $k^{\text{th}}$  channel independently of communication over any other channel. Furthermore, without knowing  $p_k(x)$ , we are likely to detect some combination of all  $N$  messages. Thus we achieve

- multiplexing of  $N$  signals,
- orthogonality of those signals
- security (the would-be code breaker must decide that this is a Fourier transform code, examine the proper range  $x_1 \leq x \leq x_2$ , and read through the proper mask), and
- jam immunity (jamming with either narrow band or broad band radiation adds only to the background but should not affect the signal modulation).

The main drawbacks are

- great complication,
- need for bright, broad band radiation sources, and
- relatively low depth of modulation and hence great power needs.

### 3.4 EXPERIMENTAL TESTS

The setup we wished to accomplish is shown in Figure 3.2. The actual setup is shown schematically in Figure 3.3. The upper part of Figure 3.3 represents the transmitter. The two interferometers of the transmitter are combined into one interferometer traversed twice by insertion of the reversing mirror  $M_x$ . Clearly, if  $M_x$  is inserted properly, all rays from the source to the output lens  $L_z$  have equal path length and no fringes appear at  $L_z$ . We were able to accomplish this with arc lamp sources (after considerable struggle). The diffuser was a device to preclude inadvertent "cheating" by passing spatial information from the mask plane (at  $M_x$ ) to the receiver. The receiver is a simple Michelson interferometer. Fringes obtained at the output (e.g. Figure 3.4) were exactly those expected for the source and geometry as calculated from the formula for  $S_m(x)$  in Sec. 3.3.

Our first attempt to modulate  $S_m(x)$  was a total failure. We then saw that our formulas and (in retrospect) common sense predicted that failure. Because these results are obvious to us only in retrospect, we believe it to be important to review them here. We attempted to modulate the envelope (visibility curve at the output) by blocking certain parts of the visibility curve with a mask in the plane of  $M_4$ . The result of this action decreased the total transmission but had no effect on the output visibility curve. It is now clear why this is true. Our masks blocked many fringes, so it obviously blocked just about as much of one wavelength as of any other. Only masks containing detail of about the size of a fringe avoid this. In order to have a significant effect on a system using light of spectral width  $\Delta\sigma$ , the length of the mask must encompass a path mismatch well in excess of the value  $1/\Delta\sigma$  needed to barely resolve that width. Thus we need a mask filling  $M_4$  with a lot of fringe-size detail in it to give good modulation. We would need to use standard integrated circuit photolithography methods to make the masks described analytically in Sec. 3.3. Therefore, we omitted the actual demonstration as well beyond our limited funding level.

### 3.5 CONCLUSION ON THE NEW METHOD

The new spectral domain spread spectrum method has been shown to work, although in a slightly more complicated way than we had anticipated.

The receiver comprises

- a double interferometer,
- $N$  predesigned spatial masks  $\xi$  aligned normal to the  $x$  direction in the spatial Fourier transform plane,
- $N$  acousto-optic modulators (one for each of the masks).

Each modulator transmits its own independent message. The outgoing beam is uniphase and spatially uniform.

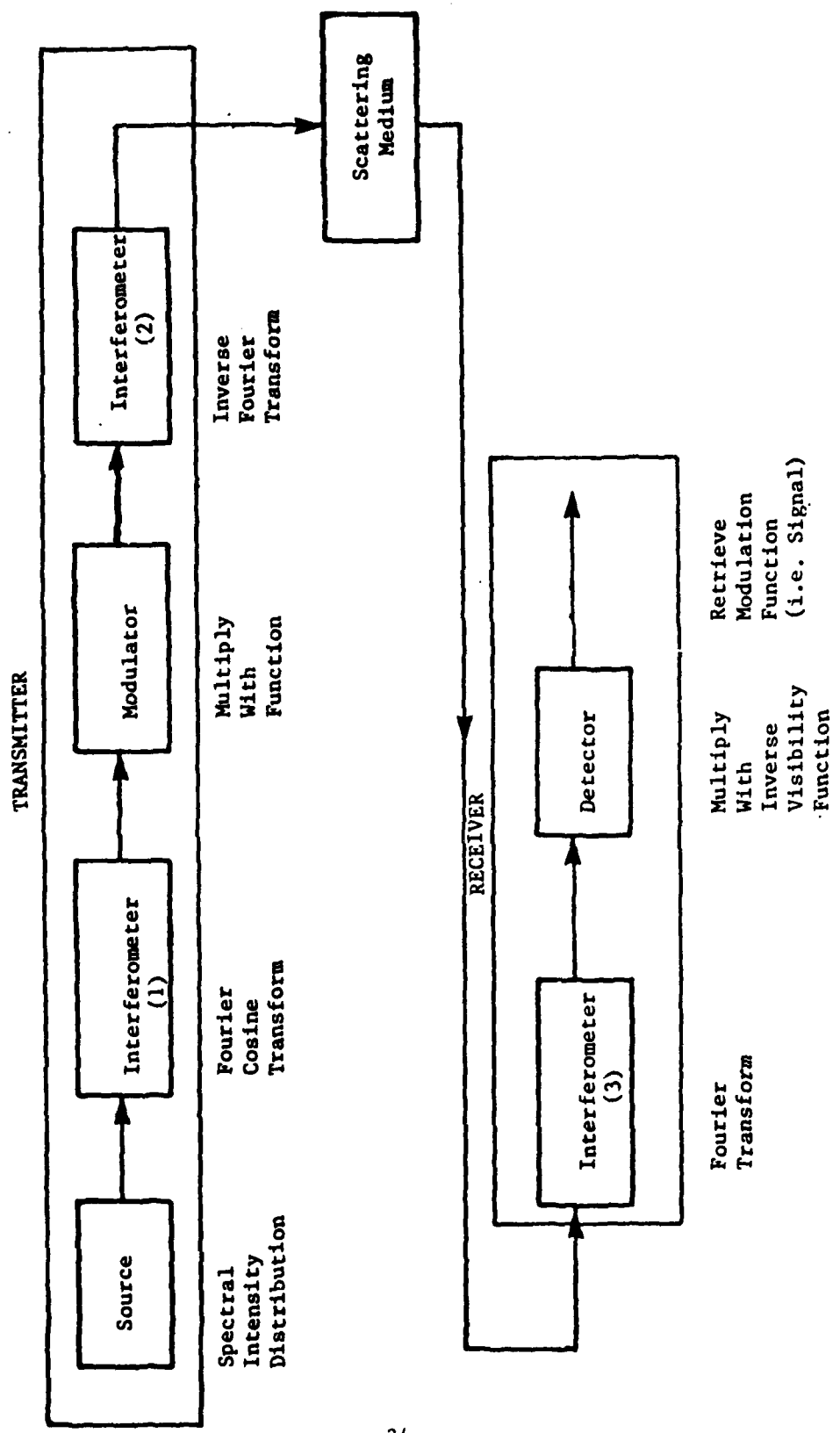


Figure 3.2 Functional Drawing of the Laboratory System

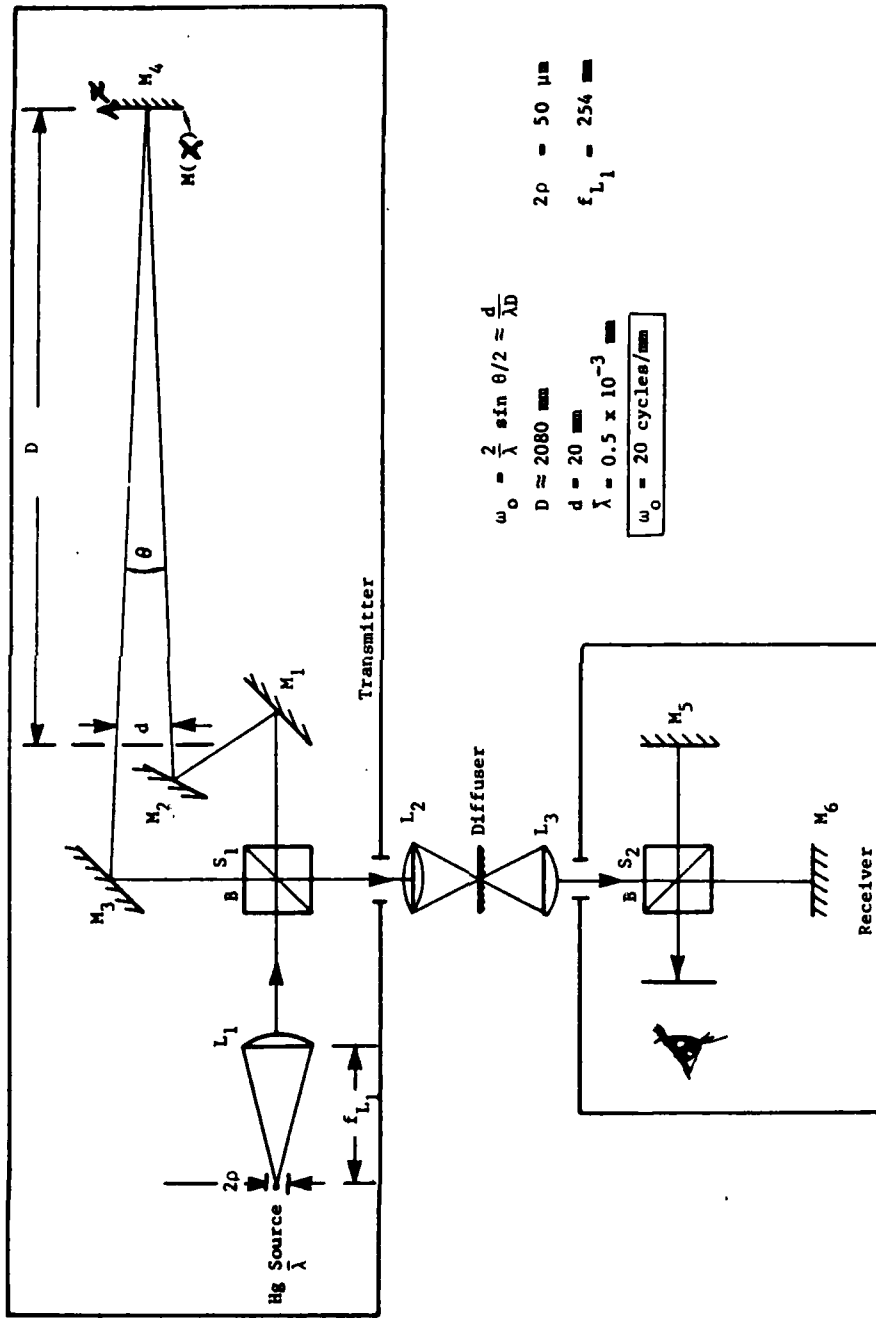


Figure 3.3 Schematic Drawing of the Laboratory System.

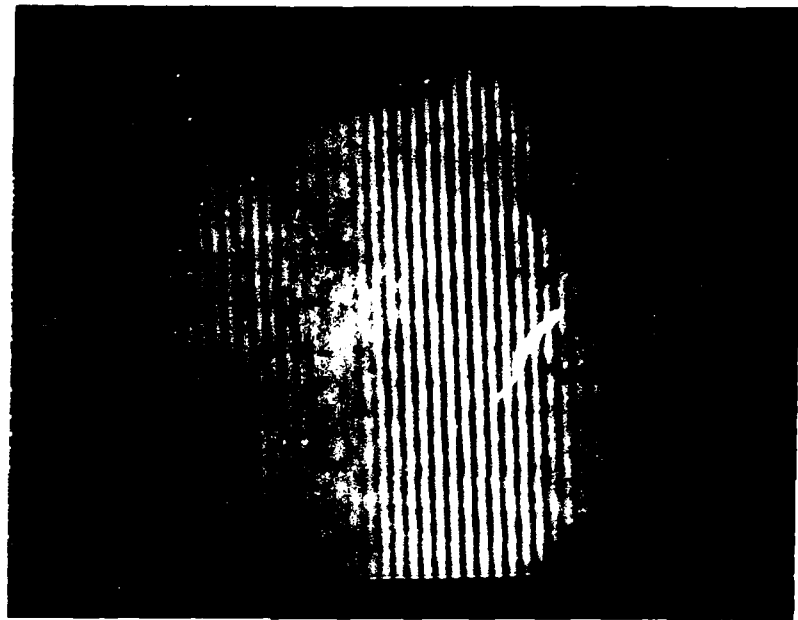


Figure 3.4 The "White light" Spectral Fourier Transform As Observed In The Spectral Filter Plane

The receiver comprises

- . N detectors (one at each N preselected location in the Fourier transform of the received spectrum).

Each detector reads the message sent by the corresponding modulator.

Many problems remain, but the basic idea is now understood and known to be both feasible and promising (for jam resistance, security, etc.).

#### 4 CONCLUSIONS

This study has led to certain definite conclusions. In particular

- (1) Optics can, in principle, be used for synchronization of very long signals even though using such signals may not be very meaningful.
- (2) For signals longer than about 1000 bits but not so long as to invoke the limitation just mentioned, optical synchronization is very appropriate.
- (3) It is feasible to do all-optical decoding of PRC SSC signals while tracking Doppler, fading, and synchronization, thus achieving significant improvements in signal-to-noise ratio.
- (4) Acousto optic tunable filters can operate at resolving powers orders of magnitude higher than previously supposed. This has important applications to Doppler tracking and to the decoding of frequency hopping systems.
- (5) Matched filtering is a special case of a far more powerful technique which we call "generalized matched filtering".
- (6) Matched filtering is a useful tool for burst-error-correcting decoding.
- (7) Fourier transform spectral multichannel transceivers have been designed to give extremely great security of communication.

The net effect of these conclusions is to emphasize the truth of our initial assumption that optics can be an important part of spread spectrum signal decoding.

## REFERENCES

1. F. A. Horrigan and W. W. Stoner. RADC-TR-78-180. August 1978.
2. J. M. Cohen and H. E. Moses, Phys., Rev. Lett. 39 1641 (1977).
3. G. Castro, D. Haarer, R. M. MacFarlane, and H. P. Tromsdorff U.S. Patent No. 4, 101, 976 (1978). A clear paper by Haarer is enclosed as an appendix.
4. E. Garmire, J. H. Marburger, S. D. Allen. Appl. Phys. Lett. 32. 320 (1978).
5. United Detector Technology, Inc. sells these.
6. I. C. Chang, Proc. SPIE 90, 12 (1977).
7. H. Kogelnik, Bell Syst. Tech. J. 48, 2909 (1969).
8. T. M. Turpin, Proc. SPIE 159, 196 (1978).
9. T. R. Bader. Appl. Opt. 18, 1668 (1979).
10. H. J. Caulfield and W. T. Maloney, Appl. Opt. 8, 2354 (1969).
11. Our program is a modified version of that of W. J. Dixon, Biomedical Computer Programs (Univ. of Calif. Press, Berkeley 1974).
12. Y-t. Chien, Interactive Pattern Recognition (Dekker, N.Y., 1979).
13. M. Born and E. Wolf, Principles of Optics, 2nd Ed., Pergamom Press. Oxford, (1960).
14. H. J. Caulfield, Opt. Eng. 13 481 (1974).
15. H. J. Caulfield, "Holographic Spectroscopy" in Advances In Holography. Vol. 2, (N.H. Farhat Ed. Dekker, N.Y.) (1976).
16. H. J. Caulfield, Opt. Commun. 23 344 (1972)